

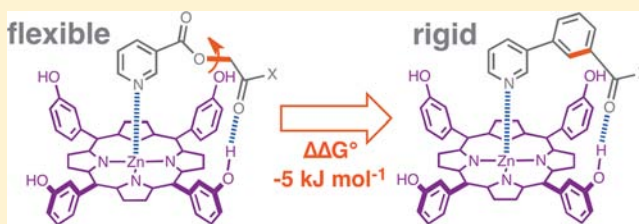
# Quantification of the Effect of Conformational Restriction on Supramolecular Effective Molarities

Harry Adams, Elena Chekmeneva, Christopher A. Hunter,\* Maria Cristina Misuraca, Cristina Navarro, and Simon M. Turega

Department of Chemistry, University of Sheffield, Sheffield S3 7HF, United Kingdom

**S** Supporting Information

**ABSTRACT:** The association constants for a family of 96 closely related zinc porphyrin–pyridine ligand complexes have been measured in two different solvents, toluene and 1,1,2,2-tetrachloroethane (TCE). The zinc porphyrin receptors are equipped with phenol side arms, which can form intramolecular H-bonds with ester or amide side arms on the pyridine ligands. These association constants were used to construct 64 chemical double mutant cycles, which measure the free energy contributions of intramolecular H-bonding interactions to the overall stability of the complexes. Measurement of association constants for the corresponding intermolecular H-bonding interactions allowed determination of the effective molarities (EM) for the intramolecular interactions. Comparison of ligands that feature amide H-bond acceptors and ester H-bonds at identical sites on the ligand framework show that the values of EM are practically identical. Similarly, the values of EM are practically identical in toluene and in TCE. However, comparison of two ligand series that differ by one degree of torsional freedom shows that the values of EM for the flexible ligands are an order of magnitude lower than for the corresponding rigid ligands. This observation holds for a range of different supramolecular architectures with different degrees of receptor–ligand complementarity and suggests that in general the cost of freezing a rotor in supramolecular complexes is of the order of 5 kJ/mol.



## INTRODUCTION

Molecular assemblies that constitute the functional elements of biological and synthetic systems are controlled by the interplay of multiple weak non-covalent interactions.<sup>1</sup> Cooperation between these interactions leads to robust structures with well-defined properties, but the nature of this cooperativity and the intrinsic properties of individual interactions can be difficult to dissect from the study of complex systems. Reliable design of new synthetic molecular assemblies will rely on the ability to make accurate predictions of the thermodynamic properties of multiple weak interactions. There has been considerable progress in estimating the contributions of specific functional group contacts to the stability of intermolecular complexes, but understanding the interplay of multiple interactions remains a challenge.<sup>2</sup>

Intramolecular interactions are more favorable than intermolecular interactions due to the unfavorable entropy associated with bimolecular processes. This effect is generally quantified by the effective molarity (EM), which is defined as the ratio of the intramolecular rate or equilibrium constant to the corresponding intermolecular rate or equilibrium constant. The relationship between EM and molecular structure has been thoroughly investigated for covalent bond formation and the values vary over many orders of magnitude.<sup>3</sup> In general, increasing the length of the linker between the two reactive ends in a covalent cyclization process decreases the rate and equilibrium constant for the cyclization reaction.<sup>4</sup> The flexibility of the linker is also important. In general, linkers with more conformational

flexibility lead to lower values of EM, and the thermodynamic advantage of freezing out a rotor, in the formation of an intramolecular covalent bond has been estimated as 5–6 kJ/mol.<sup>5</sup> Qualitatively similar results are obtained for non-covalent bond formation, which leads to the strategy of preorganization in order to maximize the stability of intermolecular complexes.

However, the variation in EM values for the formation of non-covalent bonds (supramolecular EM) is much smaller than observed for the formation of covalent bonds (covalent EM).<sup>6</sup> Increasing the length of the linker between the two non-covalent binding sites leads to a relatively small decrease in EM, and the effect of freezing out a rotor in the linker has been estimated as 0.5–5 kJ/mol.<sup>7</sup> The ability to make reasonable estimates of the likely value of EM for non-covalent interactions would be of tremendous utility in supramolecular design, where fully preorganized systems can be difficult to obtain and the interactions are sufficiently weak that small changes in EM can have a dramatic effect on the efficiency of the assembly process.<sup>8</sup> Here we describe a quantitative investigation of the influence of conformational flexibility on the magnitude of supramolecular effective molarities.

## APPROACH

We have been using complexes formed between zinc porphyrins and pyridine ligands to make a systematic quantitative investigation of the properties of intramolecular non-covalent interactions.<sup>9</sup> The

Received: October 19, 2012

Published: January 29, 2013

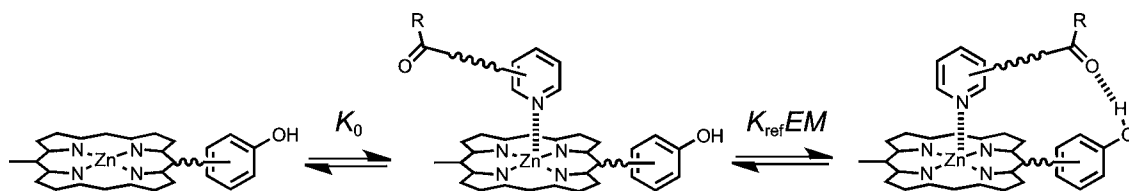


**Figure 1.** Stepwise equilibria in the formation of a porphyrin–pyridine complex containing an intramolecular H-bond.  $K_0$  is the intermolecular association constant for formation of the zinc–nitrogen interaction.  $K_{\text{ref}}EM$  is the equilibrium constant for formation of the intramolecular H-bond.  $K_{\text{ref}}$  is the equilibrium constant for formation of the corresponding intermolecular H-bond. EM is the effective molarity for the intramolecular interaction.

idea is outlined in Figure 1. Formation of a zinc pyridine coordination bond leads to formation of an intermolecular complex and peripheral groups on the porphyrin and ligand can then make intramolecular interactions. Strictly speaking the H-bond shown in Figure 1 is an intermolecular interaction, but we will use the term “intramolecular” to describe non-covalent interactions between functional groups within a molecule or within a supramolecular complex. The formation of an intramolecular interaction depends on the intrinsic strength of the interaction ( $K_{\text{ref}}$ , which is the association constant for formation of the corresponding intermolecular interaction) and the EM for the cyclization process.<sup>10</sup> If the product  $K_{\text{ref}}EM > 1$ , then the overall stability of the complex will be enhanced by the presence of the H-bonding groups, and the increase in the measured association constant can be used to determine the value of EM.

In practice, there are a number of control experiments that are required to dissect the intramolecular equilibrium constant,  $K_{\text{ref}}EM$ , from the measurement of the overall stability of the complex, and we have formalized the experiment as a chemical double mutant cycle (DMC).<sup>11</sup> Figure 2 illustrates the DMC

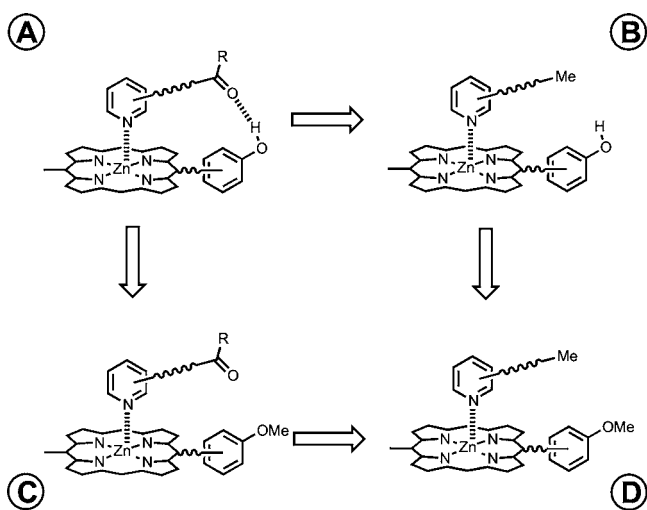


**Figure 2.** Chemical double mutant cycle (DMC) for measurement of the free energy contribution of an intramolecular H-bond to the stability of complex A.

experiment for measurement of an intramolecular H-bond in a porphyrin–ligand complex. The contribution of the H-bond to the overall stability of complex A can be estimated by measuring the stability of similar complexes where the H-bonding group on the porphyrin or ligand has been removed. However, these chemical mutations could also affect the zinc–nitrogen interaction or alter additional secondary interactions that contribute to the stability of complex A. Assuming that the contributions of pairwise

functional group interactions to the free energy change of complexation are additive, the DMC provides a straightforward method for quantifying secondary effects of the chemical mutations and dissecting out the free energy contribution from the intramolecular H-bond to the stability of complex A,  $\Delta\Delta G^\circ$  (eq 1):

$$\Delta\Delta G^\circ = \Delta G^\circ_A - \Delta G^\circ_B - \Delta G^\circ_C + \Delta G^\circ_D \quad (1)$$

This free energy can then be used to determine the value of EM, provided the association constant,  $K_{\text{ref}}$  for the corresponding intermolecular process can be determined.

We have used this approach with a family of closely related porphyrin and ligand systems to investigate the effects of changing the solvent, changing the functional groups involved in H-bond formation, and geometric complementarity on supramolecular effective molarities. The results suggest that EM is relatively insensitive to all of these parameters, with values falling in the range 1–1000 mM.<sup>9</sup> One of the striking features of the results is that changes in geometry have a relatively small impact on EM, unless the ligand is simply too short to span the H-bonding and zinc binding sites. However, the ligand systems studied to date are all relatively flexible, and here we report the effects of reducing conformational flexibility on supramolecular effective molarities.

Figure 3 illustrates two new ligand families designed to quantify the impact of the conformational restriction on

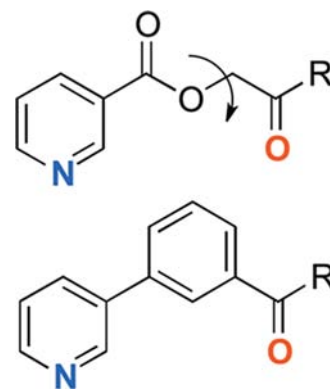


**Figure 3.** Flexible (top) and rigid (bottom) ligands. The nitrogen (blue) binds to the zinc of the porphyrin, and the carbonyl oxygen (red) can make intramolecular H-bonds with the porphyrin phenol groups. The torsion angle that is restricted on going from the flexible to the rigid ligands is highlighted.

binding affinity. These ligands will be referred to as “flexible” and “rigid” for the purposes of discussion. The key carbonyl oxygen that can make H-bonds with the porphyrin phenol groups is highlighted in red and is located at the same position on the ligand framework in both ligand families. We have shown previously that the other ester carbonyl in the flexible ligand

framework does not make H-bonds to any of the porphyrins studied here.<sup>9</sup> Comparison of EM values for related flexible and rigid ligand systems will provide a measure of the impact of conformational flexibility on binding affinity. In addition to the restriction of conformational flexibility in the rigid ligands, there are likely to be some differences in the distributions of conformations accessible to the different ligand families. The results will therefore be perturbed by variations in geometric complementarity between the porphyrin and ligand frameworks, but by studying a number of different supramolecular architectures that vary in complementarity, we hope that any important underlying preferences will emerge.

Figures 4 and 5 show the porphyrins and ligands used in this work. The porphyrins vary in the location of the phenol H-bond

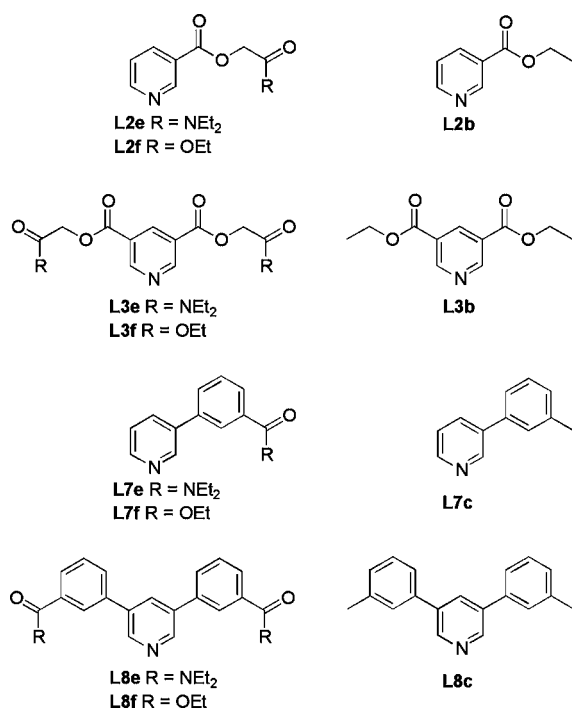


**Figure 4.** Amide ligands, L2e, L3e, L7e, and L8e; ester ligands, L2f, L3f, L7f, and L8f; and control ligands with no H-bonding groups, L2b, L3b, L7c, and L8c.

donor sites around the periphery. The ligands vary in flexibility (as illustrated in Figure 3), in the polarity of the H-bond acceptor group (ester or amide), and in the number of H-bond acceptor sites (one or two). Comparison of the one-armed and the corresponding two-armed ligands provides two independent measurements of the same intramolecular H-bond, provided there are no conformational problems in forming the doubly H-bonded complex. The experiments were carried out in two different solvents, toluene and 1,1,2,2-tetrachloroethane (TCE), which modulates the intrinsic strength of the H-bond interaction. This set of porphyrins, ligands, and solvents can be used to measure EM for 64 different supramolecular systems, and comparison of the flexible and rigid ligand results provides a clear picture of the effect of conformational flexibility on binding affinity.

## RESULTS AND DISCUSSION

**Synthesis.** Synthesis of the porphyrin receptors and control ligands L2b and L3b was carried out as described previously.<sup>9</sup> The ligands with flexible linkers were synthesized from the corresponding carboxylic acids **1** and **2** via the acid chlorides.

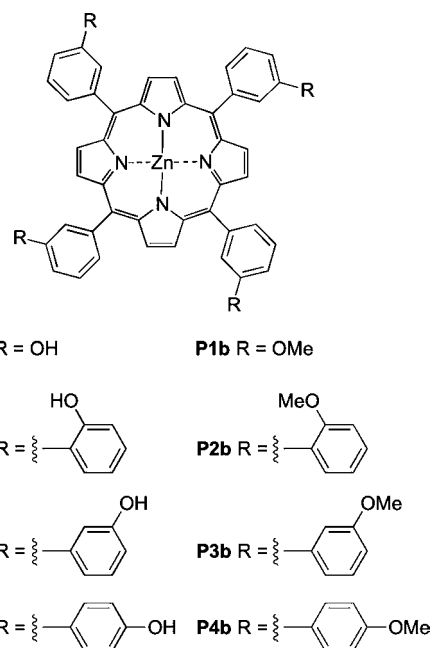
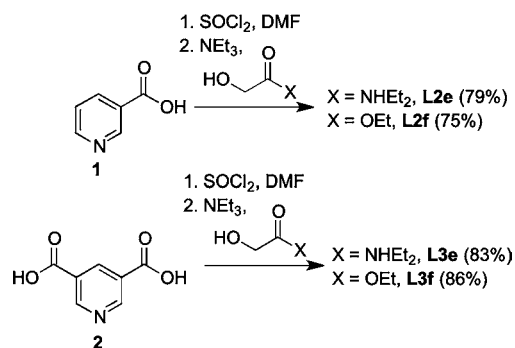


**Figure 5.** Porphyrin receptors, P1a–P4a (R = OH) and P1b–P4b (R = OMe).

Coupling of the acid chlorides with *N,N*-diethyl-2-hydroxyacetamide gave amides L2e and L3e, and coupling with ethyl glycolate gave esters L2f and L3f in reasonable yields (Scheme 1).<sup>9</sup>

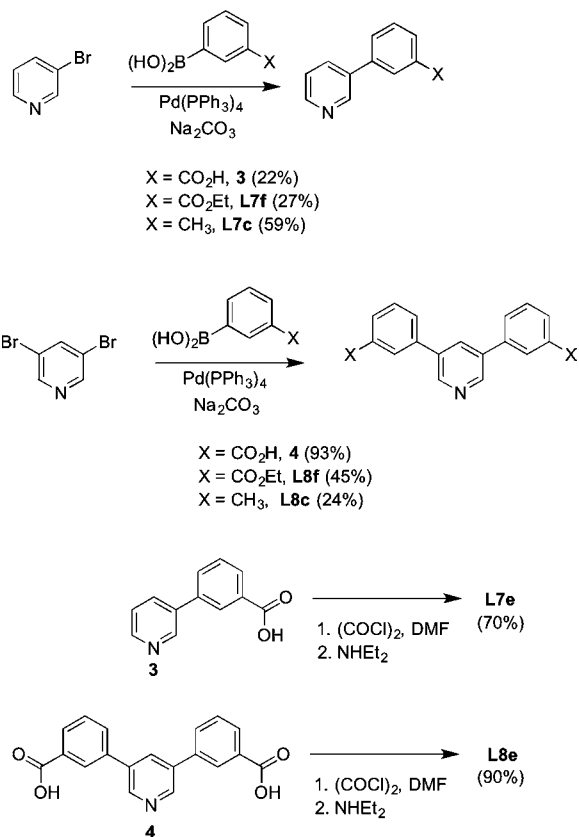
### Scheme 1. Synthesis of Flexible Ligands



The rigid ester ligands L7f and L8f were synthesized using palladium-catalyzed Suzuki–Morita cross-coupling of 3-ethoxycarbonylphenylboronic acid with 3-bromopyridine and 3,5-bromopyridine, respectively (Scheme 2).<sup>12</sup> The rigid amide ligands were synthesized in two steps. Suzuki–Morita cross-coupling of 3-carboxyphenylboronic acid with 3-bromopyridine and 3,5-bromopyridine gave carboxylic acids **3** and **4**, respectively (Scheme 2). Each acid was converted to the acid chloride and coupled with diethylamine to give ligands L7e and L8e (Scheme 2). Control ligands L7c and L8c were synthesized from 3-bromopyridine and 3,5-bromopyridine by Suzuki–Morita coupling with 3-methylphenylboronic acid (Scheme 2).

**High-Throughput Titration Analysis of Binding.** The association constants for the 96 different complexes formed by all pairwise combinations of the 12 ligands and 8 zinc porphyrins were measured using UV/vis absorption titrations in toluene and in TCE. The porphyrin Soret band undergoes a large shift on complexation of the zinc with a pyridine ligand, and this provides a convenient spectroscopic probe to monitor

## Scheme 2. Synthesis of Rigid Ligands



binding. Titrations were carried out using automated protocols on a UV/vis plate reader, providing a convenient method for collecting a large amount of quantitative data.

In most cases, the data fit well to a 1:1 binding isotherm, and the association constants are reported in Tables 1 and 2 for toluene and TCE, respectively. However, some of the complexes are too stable allow accurate measurement of association constants using UV/vis absorption spectroscopy ( $K > 10^6 \text{ M}^{-1}$ ). In these cases, fluorescence spectroscopy or isothermal titration calorimetry (ITC) was used to measure the association constant. Again the data fit well to a 1:1 binding isotherm, and the results are included in Tables 1 and 2. In cases where association constants could be measured by more

than one technique, the results are the same within error. For example, the **P1a**·**L7f** association constant measured by UV/vis absorption titrations was  $(1.8 \pm 0.1) \times 10^6 \text{ M}^{-1}$ , compared with  $(2.3 \pm 0.8) \times 10^6 \text{ M}^{-1}$  measured by ITC.

Figure 6 compares the association constants measured in toluene with the results in TCE. As we have found previously in related systems, the complexes are more stable by 1–2 orders of magnitude in the less polar solvent, toluene.<sup>9</sup> There is a reasonable correlation between the two data sets, indicating that the complexes that are more stable in toluene are generally more stable in TCE, but the scatter in Figure 6 shows that the relative stabilities of the complexes are altered by changes in solvation.

**DMC Analysis of Intramolecular H-Bonding.** The data in Tables 1 and 2 are illustrated graphically in Figure 7, with the complexes organized and colored according to their role in the DMC. The complexes that can make intramolecular H-bonds (blue) are generally more stable than the complexes that cannot, and the increase in stability is larger for the amide ligands (pale blue) than for the ester ligands (dark blue). The free energy contributions due to intramolecular H-bonding interactions,  $\Delta\Delta G^\circ$ , were determined using the data in Tables 1 and 2 in eq 1, and the results are presented in Tables 3–6.

In toluene, 14 of the 16 amide complexes make detectable H-bonding interactions with free energy contributions of up to 21 kJ/mol to the overall stability of the complex. The ester H-bonds are significantly weaker and contribute less than 10 kJ/mol to the overall stability of the complexes in all cases. In TCE, the free energy contributions from H-bonding are reduced somewhat, because this solvent is more polar, and there is a larger desolvation penalty for H-bond formation.

Figure 8 shows the relationship between the free energy contributions due to H-bonding in the one-armed and two-armed ligands. An assumption of the DMC analysis is that free energy contributions from individual intermolecular interactions are additive. The two-armed ligands are symmetrical, so if this assumption is correct, then the value of  $\Delta\Delta G^\circ$  for the two-armed ligands should be double the value for the corresponding one-armed ligand. Figure 8 shows that in general this is indeed the case. There is one outlier in Figure 8, the **P1a**·**L7e**/**L8e** complex in toluene. This is the complex that makes the strongest H-bonding interactions, and it is possible that there is a conformational issue that prevents formation of two optimal interactions simultaneously. However, additive behavior is observed for this complex in TCE.

Table 1. Association Constants ( $K$ ,  $\text{M}^{-1}$ ) for the Formation of 1:1 Complexes in Toluene at 298 K (with Percentage Errors)

ligand	porphyrin							
	P1a	P2a	P3a	P4a	P1b	P2b	P3b	P4b
L2e	$9.6 \times 10^4$ (10%)	$1.4 \times 10^4$ (7%)	$6.6 \times 10^4$ (3%)	$3.2 \times 10^3$ (20%)	$2.2 \times 10^3$ (40%)	$1.5 \times 10^3$ (8%)	$3.6 \times 10^3$ (10%)	$2.4 \times 10^3$ (20%)
L3e	$2.8 \times 10^6$ (40%)	$4.0 \times 10^4$ (8%)	$2.9 \times 10^5$ (30%)	$2.3 \times 10^3$ (40%)	$2.0 \times 10^3$ (30%)	$8.9 \times 10^2$ (6%)	$3.0 \times 10^3$ (3%)	$2.2 \times 10^3$ (5%)
L7e	$1.3 \times 10^6$ (20%)	$1.8 \times 10^5$ (20%)	$7.4 \times 10^5$ (8%)	$2.6 \times 10^4$ (10%)	$7.2 \times 10^3$ (1%)	$5.6 \times 10^3$ (4%)	$9.3 \times 10^3$ (2%)	$9.6 \times 10^3$ (5%)
L8e	$2.6 \times 10^7$ (20%) <sup>a</sup>	$2.0 \times 10^6$ (40%) <sup>a</sup>	$8.2 \times 10^6$ (10%) <sup>a</sup>	$9.7 \times 10^4$ (30%)	$7.4 \times 10^3$ (7%)	$5.1 \times 10^3$ (20%)	$9.7 \times 10^3$ (9%)	$1.1 \times 10^4$ (6%)
L2f	$6.5 \times 10^3$ (30%)	$3.4 \times 10^3$ (1%)	$7.4 \times 10^3$ (4%)	$3.0 \times 10^3$ (7%)	$2.3 \times 10^3$ (40%)	$1.6 \times 10^3$ (10%)	$3.5 \times 10^3$ (6%)	$2.9 \times 10^3$ (20%)
L3f	$1.2 \times 10^4$ (5%)	$2.4 \times 10^3$ (30%)	$8.5 \times 10^3$ (20%)	$2.3 \times 10^3$ (10%)	$2.2 \times 10^3$ (10%)	$1.1 \times 10^3$ (20%)	$3.6 \times 10^3$ (10%)	$2.3 \times 10^3$ (20%)
L7f	$4.1 \times 10^4$ (20%)	$1.5 \times 10^4$ (20%)	$2.0 \times 10^4$ (5%)	$1.1 \times 10^4$ (9%)	$7.5 \times 10^3$ (1%)	$6.3 \times 10^3$ (1%)	$1.1 \times 10^4$ (1%)	$1.0 \times 10^4$ (5%)
L8f	$2.7 \times 10^5$ (7%)	$1.3 \times 10^4$ (5%)	$2.8 \times 10^4$ (10%)	$1.6 \times 10^4$ (6%)	$9.3 \times 10^3$ (3%)	$6.6 \times 10^3$ (3%)	$1.6 \times 10^4$ (4%)	$1.4 \times 10^4$ (5%)
L2b	$3.6 \times 10^3$ (8%)	$5.1 \times 10^3$ (2%)	$8.5 \times 10^3$ (1%)	$5.1 \times 10^3$ (6%)	$3.9 \times 10^3$ (20%)	$3.3 \times 10^3$ (6%)	$6.2 \times 10^3$ (30%)	$5.4 \times 10^3$ (4%)
L3b	$3.2 \times 10^3$ (1%)	$4.3 \times 10^3$ (5%)	$6.9 \times 10^3$ (9%)	$5.1 \times 10^3$ (40%)	$3.8 \times 10^3$ (20%)	$2.6 \times 10^3$ (10%)	$6.0 \times 10^3$ (20%)	$4.5 \times 10^3$ (20%)
L7c	$8.0 \times 10^3$ (30%)	$1.3 \times 10^4$ (3%)	$1.8 \times 10^4$ (10%)	$1.3 \times 10^4$ (1%)	$8.8 \times 10^3$ (1%)	$7.3 \times 10^3$ (4%)	$1.3 \times 10^4$ (20%)	$1.1 \times 10^4$ (5%)
L8c	$1.0 \times 10^4$ (3%)	$1.4 \times 10^4$ (7%)	$2.5 \times 10^4$ (10%)	$1.9 \times 10^4$ (4%)	$1.4 \times 10^4$ (7%)	$9.0 \times 10^3$ (10%)	$2.4 \times 10^4$ (4%)	$1.8 \times 10^4$ (10%)

<sup>a</sup>Measured using ITC.

Table 2. Association Constants ( $K$ ,  $M^{-1}$ ) for the Formation of 1:1 Complexes in TCE at 298 K (with Percentage Errors)

ligand	porphyrin							
	P1a	P2a	P3a	P4a	P1b	P2b	P3b	P4b
L2e	$1.2 \times 10^4$ (8%)	$1.3 \times 10^3$ (3%)	$2.9 \times 10^3$ (3%)	$3.6 \times 10^2$ (10%)	$4.0 \times 10^2$ (30%)	$2.3 \times 10^2$ (4%)	$3.8 \times 10^2$ (8%)	$4.0 \times 10^2$ (3%)
L3e	$7.0 \times 10^4$ (3%)	$6.7 \times 10^2$ (1%)	$3.1 \times 10^3$ (3%)	$1.6 \times 10^2$ (4%)	$1.3 \times 10^2$ (6%)	$7.3 \times 10^1$ (5%)	$7.4 \times 10^1$ (30%)	$9.0 \times 10^1$ (10%)
L7e	$1.1 \times 10^5$ (30%)	$1.5 \times 10^4$ (1%)	$4.1 \times 10^4$ (4%)	$2.4 \times 10^3$ (3%)	$2.0 \times 10^3$ (20%)	$1.5 \times 10^3$ (3%)	$1.9 \times 10^3$ (5%)	$1.7 \times 10^3$ (4%)
L8e	$3.7 \times 10^6$ (20%) <sup>a</sup>	$3.1 \times 10^4$ (10%)	$2.8 \times 10^5$ (1%)	$2.3 \times 10^3$ (9%)	$1.1 \times 10^3$ (20%)	$8.0 \times 10^2$ (10%)	$1.1 \times 10^3$ (9%)	$1.1 \times 10^3$ (6%)
L2f	$1.5 \times 10^3$ (5%)	$7.9 \times 10^2$ (4%)	$1.0 \times 10^3$ (3%)	$4.0 \times 10^2$ (5%)	$3.9 \times 10^2$ (5%)	$2.2 \times 10^2$ (9%)	$4.1 \times 10^2$ (10%)	$4.4 \times 10^2$ (7%)
L3f	$1.1 \times 10^3$ (30%)	$2.3 \times 10^2$ (4%)	$4.1 \times 10^2$ (10%)	$1.1 \times 10^2$ (9%)	$9.1 \times 10^1$ (8%)	$7.5 \times 10^1$ (3%)	$1.2 \times 10^2$ (7%)	$8.7 \times 10^1$ (9%)
L7f	$1.6 \times 10^4$ (10%)	$3.9 \times 10^3$ (3%)	$3.3 \times 10^3$ (3%)	$2.3 \times 10^3$ (4%)	$2.1 \times 10^3$ (10%)	$1.8 \times 10^3$ (6%)	$2.3 \times 10^3$ (4%)	$2.0 \times 10^3$ (5%)
L8f	$8.8 \times 10^4$ (5%)	$2.7 \times 10^3$ (3%)	$3.3 \times 10^3$ (6%)	$1.9 \times 10^3$ (10%)	$1.3 \times 10^3$ (20%)	$1.2 \times 10^3$ (8%)	$1.6 \times 10^3$ (10%)	$1.6 \times 10^3$ (4%)
L2b	$1.5 \times 10^3$ (30%)	$1.8 \times 10^3$ (6%)	$1.7 \times 10^3$ (20%)	$1.3 \times 10^3$ (30%)	$1.1 \times 10^3$ (9%)	$9.0 \times 10^2$ (9%)	$1.2 \times 10^3$ (8%)	$1.1 \times 10^3$ (20%)
L3b	$7.0 \times 10^2$ (10%)	$6.7 \times 10^2$ (20%)	$7.1 \times 10^2$ (7%)	$4.7 \times 10^2$ (4%)	$4.0 \times 10^2$ (20%)	$3.2 \times 10^2$ (6%)	$3.7 \times 10^2$ (10%)	$3.5 \times 10^2$ (6%)
L7c	$4.1 \times 10^3$ (2%)	$4.5 \times 10^3$ (4%)	$4.0 \times 10^3$ (2%)	$3.2 \times 10^3$ (9%)	$3.0 \times 10^3$ (1%)	$2.4 \times 10^3$ (4%)	$3.3 \times 10^3$ (2%)	$2.8 \times 10^3$ (7%)
L8c	$5.1 \times 10^3$ (10%)	$5.4 \times 10^3$ (4%)	$5.5 \times 10^3$ (4%)	$4.6 \times 10^3$ (4%)	$3.2 \times 10^3$ (3%)	$2.4 \times 10^3$ (2%)	$3.6 \times 10^3$ (3%)	$3.4 \times 10^3$ (9%)

<sup>a</sup>Measured using fluorescence spectroscopy.

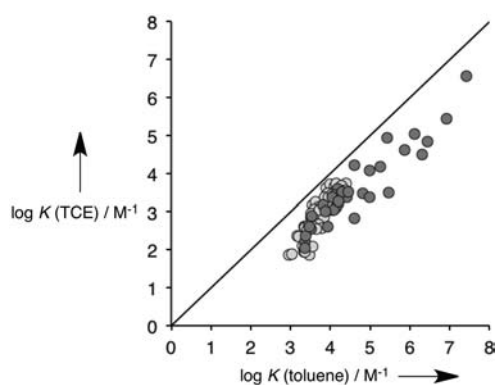


**Figure 6.** Comparison of the 1:1 association constants ( $\log K/M^{-1}$ ) for formation of porphyrin–ligand complexes in TCE with the corresponding values measured in toluene. Data for the complexes that can make intramolecular H-bonds are shown in dark gray, and data for control complexes are shown in pale gray. The line corresponds to  $\log K(\text{TCE}) = \log K(\text{toluene})$ .

Figure 9 compares the values of  $\Delta\Delta G^\circ$  for rigid ligands with the values measured for the corresponding flexible ligands. In

**Table 3.** Free Energy Contributions from Amide–Phenol H-Bonds at 298 K in Toluene ( $\Delta\Delta G^\circ$ , kJ/mol) Determined Using the Chemical Double Mutant Cycle in Figure 2<sup>a</sup>

porphyrin	ligand			
	L2e	L3e	L7e	L8e
P1a	–10	–18	–13	–21
P2a	–4	–8	–7	–14
P3a	–6	–11	–10	–17
P4a	–1	0	–2	–5

<sup>a</sup>Average error over the data set  $\pm 1$  kJ/mol. Complexes that do not make detectable H-bonds are in italics ( $\Delta\Delta G^\circ > -2$  kJ/mol).

all cases, the H-bonds formed by the rigid ligands are more favorable than those formed by the flexible ligands with differences of up to 6 kJ/mol. These differences are a measure of the effects of preorganization of the ligand framework on binding affinity. However, the variations in  $\Delta\Delta G^\circ$  contain contributions that vary with the solvent, with the functional groups involved in the H-bond, and with the geometric complementarity of the ligand–porphyrin architecture. To account for the contributions due to solvent and H-bond

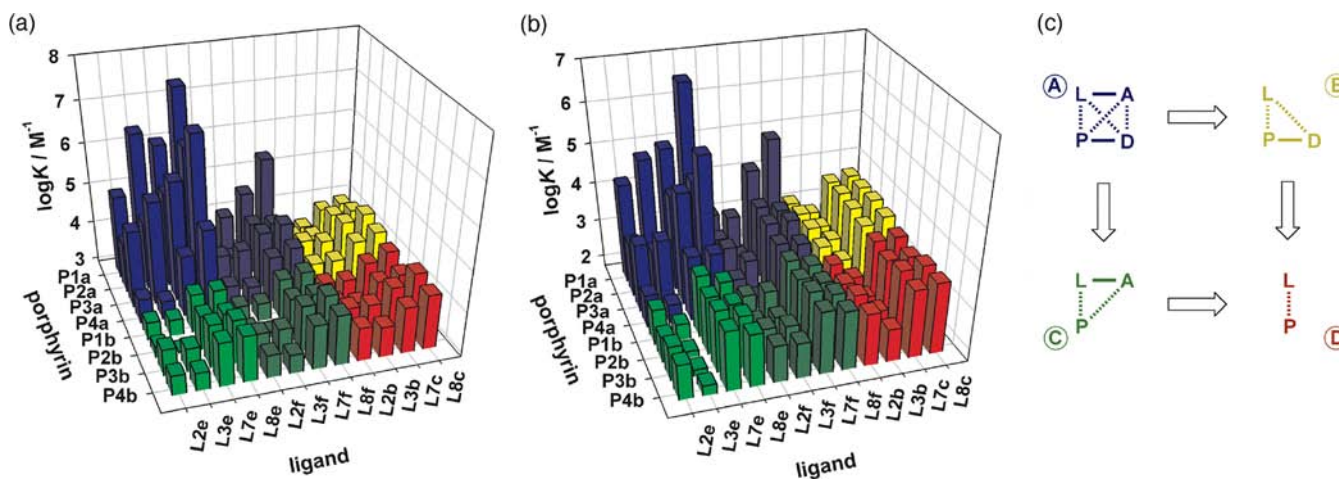


**Figure 7.** Association constants ( $\log K/M^{-1}$ ) measured in (a) toluene and (b) TCE. (c) Schematic representation of the chemical DMC used to extract information on the magnitude of the intramolecular H-bond interaction between A and D in the complex formed between a zinc porphyrin (P) and a pyridine ligand (L). Data for the amide ligand–hydroxyporphyrin complexes are shown in blue, amide ligand–methoxyporphyrin complexes in green, ester ligand–hydroxyporphyrin complexes in dark blue, ester ligand–methoxyporphyrin complexes in dark green, control ligand–hydroxyporphyrin complexes in yellow, and control ligand–methoxyporphyrin complexes in red.

**Table 4. Free Energy Contributions from Amide–Phenol H-Bonds at 298 K in TCE ( $\Delta\Delta G^\circ$ , kJ/mol) Determined Using the Chemical Double Mutant Cycle in Figure 2<sup>a</sup>**

porphyrin	ligand			
	L2e	L3e	L7e	L8e
P1a	–8	–14	–9	–19
P2a	–3	–4	–4	–7
P3a	–4	–8	–7	–13
P4a	<i>1</i>	<i>–1</i>	<i>–1</i>	<i>–1</i>

<sup>a</sup>Average error over the data set  $\pm 1$  kJ/mol. Complexes that do not make detectable H-bonds are in italics ( $\Delta\Delta G^\circ > -2$  kJ/mol).

**Table 5. Free Energy Contributions from Ester–Phenol H-Bonds at 298 K in Toluene ( $\Delta\Delta G^\circ$ , kJ/mol) Determined Using the Chemical Double Mutant Cycle in Figure 2<sup>a</sup>**

porphyrin	ligand			
	L2f	L3f	L7f	L8f
P1a	–3	–5	–4	–9
P2a	–1	–1	–1	–1
P3a	–1	–2	–1	–1
P4a	<i>0</i>	<i>0</i>	<i>0</i>	<i>0</i>

<sup>a</sup>Average error over the data set  $\pm 1$  kJ/mol. Complexes that do not make detectable H-bonds are in italics ( $\Delta\Delta G^\circ > -2$  kJ/mol).

**Table 6. Free Energy Contributions from Ester–Phenol H-Bonds at 298 K in TCE ( $\Delta\Delta G^\circ$ , kJ/mol) Determined Using the Chemical Double Mutant Cycle in Figure 2<sup>a</sup>**

porphyrin	ligand			
	L2f	L3f	L7f	L8f
P1a	–3	–5	–4	–9
P2a	–1	–1	<i>0</i>	<i>0</i>
P3a	–1	–1	<i>0</i>	–1
P4a	<i>1</i>	<i>0</i>	<i>0</i>	<i>0</i>

<sup>a</sup>Average error over the data set  $\pm 1$  kJ/mol. Complexes that do not make detectable H-bonds are in italics ( $\Delta\Delta G^\circ > -2$  kJ/mol).

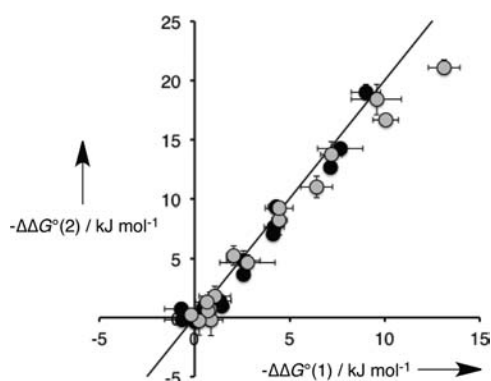


**Figure 8.** Total free energy contribution due to intramolecular H-bonding for ligands with two identical side arms,  $\Delta\Delta G^\circ(2)$ , compared with data for the corresponding one-armed ligands,  $\Delta\Delta G^\circ(1)$ , in toluene (gray) and TCE (black). The line corresponds to  $\Delta\Delta G^\circ(2) = 2\Delta\Delta G^\circ(1)$ .

strength, it is necessary to compare the effective molarities (EM) for the intramolecular interactions.

In order to determine the values of EM for the intramolecular H-bonds, association constants for the corresponding intermolecular interactions,  $K_{\text{ref}}$  were measured. The compounds

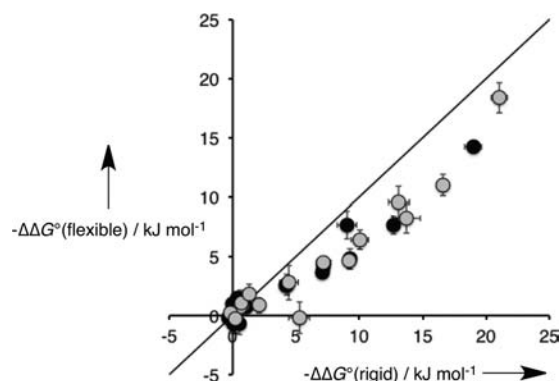


**Figure 9.** Total free energy contribution due to intramolecular H-bonding for rigid ligands,  $\Delta\Delta G^\circ(\text{rigid})$ , compared with data for the corresponding flexible ligands,  $\Delta\Delta G^\circ(\text{flexible})$ , in toluene (gray) and TCE (black). The line corresponds to  $\Delta\Delta G^\circ(\text{flexible}) = \Delta\Delta G^\circ(\text{rigid})$ .

used are shown in Figure 10. Association constants for the interaction of *p*-cresol with aliphatic and aromatic esters and

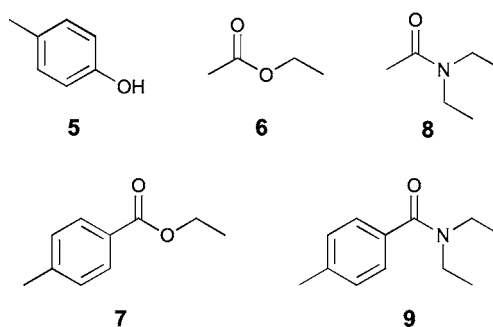


**Figure 10.** Compounds used to quantify intermolecular H-bond interactions.

amides were measured using <sup>1</sup>H NMR titrations in toluene and in TCE, and the results are shown in Table 7.

The results are consistent with the observations made for the intramolecular interactions in the porphyrin–ligand complexes. The amide–phenol H-bonds are stronger than the ester–phenol H-bonds, and the interactions are marginally weaker in TCE than in toluene. There are also substituent effects: the aliphatic amide and ester groups of the flexible ligands are slightly better H-bond acceptors than the aromatic groups on the rigid ligands. The ester complexes are not sufficiently stable for accurate measurement of small differences, but there is a two-fold difference between the stabilities of the aromatic and aliphatic amide–phenol complexes. Table 7 compares the measured association constants with the values predicted using literature H-bond parameters in eq 2,<sup>2e</sup>

$$-RT \ln K_{\text{calc}} = -(\alpha_{\text{D}} - \alpha_{\text{S}})(\beta_{\text{A}} - \beta_{\text{S}}) + 6 \text{ kJ/mol} \quad (2)$$

where  $K_{\text{calc}}$  is the intermolecular association constant at  $T = 298$  K,  $\alpha_{\text{D}}$  and  $\beta_{\text{A}}$  are the H-bond parameters of the H-bond donor (D) and H-bond acceptor (A),  $\alpha_{\text{S}}$  and  $\beta_{\text{S}}$  are the H-bond donor and acceptor parameters of the solvent, and the constant of 6 kJ/mol was experimentally determined in carbon tetrachloride solution but is assumed to apply to all organic solvents. There is good agreement in Table 7, and this gives some confidence that the small association constants measured for the ester complexes are reliable.

**Table 7. Association Constants ( $K/M^{-1}$ ) for the Formation of H-Bonded Complexes at 298 K Measured by  $^1\text{H}$  NMR Titrations ( $K_{\text{expt}}$ ) and Estimated Using Eq 2 ( $K_{\text{calc}}$ )<sup>a</sup>**

complex	solvent	$\alpha$	$\beta$	$\alpha_s$	$\beta_s$	$K_{\text{expt}}$	$K_{\text{calc}}$
5•6	toluene	3.8	5.4	1.0	2.2	$3 \pm 1$	3
5•7	toluene	3.8	5.1	1.0	2.2	$3 \pm 1$	2
5•8	toluene	3.8	8.5	1.0	2.2	$86 \pm 20$	110
5•9	toluene	3.8	7.9	1.0	2.2	$33 \pm 1$	54
5•6	TCE	3.8	5.4	2.0	1.3	$2 \pm 1$	2
5•7	TCE	3.8	5.1	2.0	1.3	$2 \pm 1$	1
5•8	TCE	3.8	8.5	2.0	1.3	$22 \pm 3$	16
5•9	TCE	3.8	7.9	2.0	1.3	$11 \pm 2$	11

<sup>a</sup>H-bond parameters from ref 13.

The observed association constant for the formation of a zinc porphyrin–pyridine complex containing an intramolecular H-bond can be described in terms of  $K_0$ , the zinc–nitrogen interaction, and  $K_{\text{ref}}\text{EM}$ , the equilibrium constant for the formation of the intramolecular H-bond (Figure 1).<sup>9</sup> When  $K_{\text{ref}}\text{EM} \gg 1$ , the H-bonded state is fully populated, but if  $K_{\text{ref}}\text{EM} \leq 1$ , then partially bound states, where the H-bond is not formed, must also be considered. The observed association constant  $K_{\text{obs}}$  is the sum of the association constants for all partially and fully bound states. Where a single intramolecular H-bond is possible,  $K_{\text{obs}}$  is given by eq 3,

$$K_{\text{obs}} = K_0 + K_0 K_{\text{ref}} \text{EM} = K_0(1 + K_{\text{ref}} \text{EM}) \quad (3)$$

For the porphyrin–ligand complexes considered here, there are multiple H-bonding sites, so a statistical factor that accounts for the degeneracy of the complex must be included. For the one-armed ligand complexes, there are four possible H-bonding interactions that can be formed, and the value of  $K_{\text{obs}}$  is given by eq 4,

$$K_{\text{obs}} = K_0(1 + 4K_{\text{ref}} \text{EM}) \quad (4)$$

For the rigid two-armed ligand complexes, we assume that the value of EM for formation of the first H-bond is the same as EM for formation of the second H-bond. This is supported by the additive free energy increments observed for the one-armed and two-armed ligands (Figure 8). The value of  $K_{\text{obs}}$  is therefore given by eq 5,

$$K_{\text{obs}} = K_0(1 + 8K_{\text{ref}} \text{EM} + 4(K_{\text{ref}} \text{EM})^2) \quad (5)$$

For the flexible two-armed ligand complexes, the value of  $K_{\text{obs}}$  is given by eq 6.

$$K_{\text{obs}} = K_0(1 + 8K_{\text{ref}} \text{EM} + 8(K_{\text{ref}} \text{EM})^2) \quad (6)$$

The statistical factors used for the rigid and flexible two-armed ligands differ, because ligand flexibility alters the number of different fully bound complexes that can be formed. Models show that the flexible ligand can make two H-bonds with both the *cis*- and the *trans*-related *meso*-phenol substituents on the porphyrin receptors. In contrast, the rigid ligand can only interact simultaneously with the *trans* substituents. This is confirmed by an X-ray crystal structure of the **P1a**•**L8f** complex (Figure 11).

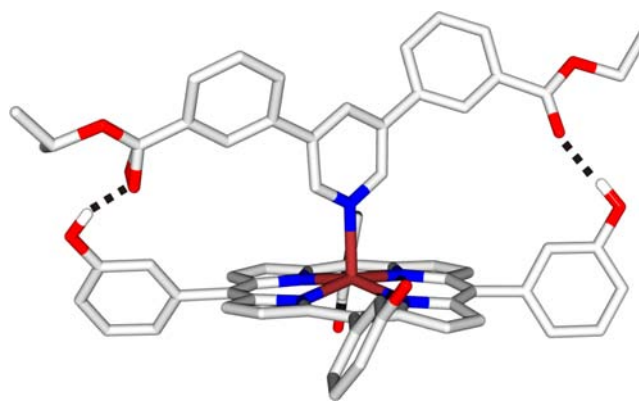


**Figure 11.** Crystal structure of the **P1a**•**L8f** complex showing the fully bound state with two H-bonds between the ester substituents on the ligand and the *trans*-related *meso*-phenol groups on the porphyrin. Hydrogen atoms not involved in H-bonding, and two DCM molecules are omitted for clarity. One of the ester carbonyl oxygen atoms is disordered over two sites that are very close in space.

In the DMC, any differences in  $K_0$  cancel, so the values of  $K_{\text{ref}}$  in Table 7 can be used to calculate the values of EM from the  $\Delta\Delta G^\circ$  values in Tables 3–6 as follows. For the one-armed ligand complexes,

$$e^{-\Delta\Delta G^\circ/RT} = 1 + 4K_{\text{ref}} \text{EM} \quad (7)$$

For the rigid two-armed ligand complexes,

$$e^{-\Delta\Delta G^\circ/RT} = 1 + 8K_{\text{ref}} \text{EM} + 4(K_{\text{ref}} \text{EM})^2 \quad (8)$$

For the flexible two-armed ligand complexes,

$$e^{-\Delta\Delta G^\circ/RT} = 1 + 8K_{\text{ref}} \text{EM} + 8(K_{\text{ref}} \text{EM})^2 \quad (9)$$

Solving these equations for EM gives the results reported in Tables 8–11.

**Table 8. Effective Molarities (EM, mM) for Intramolecular Amide–Phenol H-Bonds Measured at 298 K in Toluene<sup>a</sup>**

porphyrin	ligand			
	L2e	L3e	L7e	L8e
P1a	140	130	1500	1000
P2a	15	14	130	210
P3a	36	27	430	400
P4a	<i>b</i>	<i>b</i>	10	20

<sup>a</sup>Average error over the data set  $\pm 50\%$ . <sup>b</sup>No interaction detected.

**Table 9. Effective Molarities (EM, mM) for Intramolecular Amide–Phenol H-Bonds Measured at 298 K in TCE<sup>a</sup>**

porphyrin	ligand			
	L2e	L3e	L7e	L8e
P1a	240	220	890	2000
P2a	21	13	98	110
P3a	50	47	380	500
P4a	<i>b</i>	<i>b</i>	<i>b</i>	<i>b</i>

<sup>a</sup>Average error over the data set  $\pm 50\%$ . <sup>b</sup>No interaction detected.

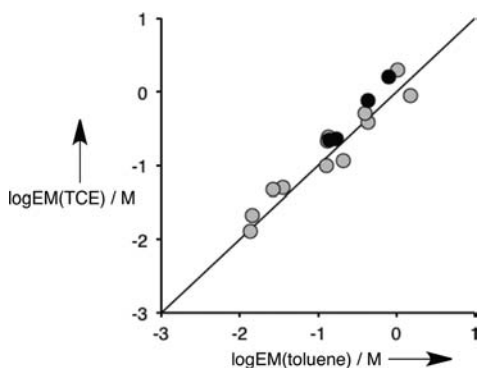
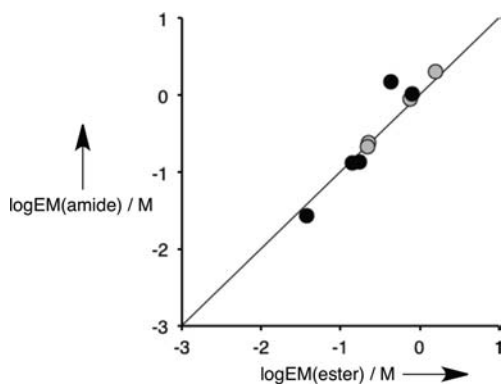
The values of EM show considerable variation with the supramolecular architecture of the complex and range from 10 mM to 2 M. Figure 12 compares the values of EM measured in toluene with the corresponding values measured in TCE.

**Table 10.** Effective Molarities (EM, mM) for Intramolecular Ester–Phenol H-Bonds Measured at 298 K in Toluene<sup>a</sup>

porphyrin	ligand			
	L2f	L3f	L7f	L8f
P1a	170	140	430	790
P2a	<i>b</i>	<i>b</i>	<i>b</i>	<i>b</i>
P3a	<i>b</i>	38	<i>b</i>	<i>b</i>
P4a	<i>b</i>	<i>b</i>	<i>b</i>	<i>b</i>

<sup>a</sup>Average error over the data set  $\pm 50\%$ . <sup>b</sup>No interaction detected.**Table 11.** Effective molarities (EM, mM) for Intramolecular Ester–Phenol H-Bonds Measured at 298 K in TCE<sup>a</sup>

porphyrin	ligand			
	L2f	L3f	L7f	L8f
P1a	230	220	760	1600
P2a	<i>b</i>	<i>b</i>	<i>b</i>	<i>b</i>
P3a	<i>b</i>	<i>b</i>	<i>b</i>	<i>b</i>
P4a	<i>b</i>	<i>b</i>	<i>b</i>	<i>b</i>

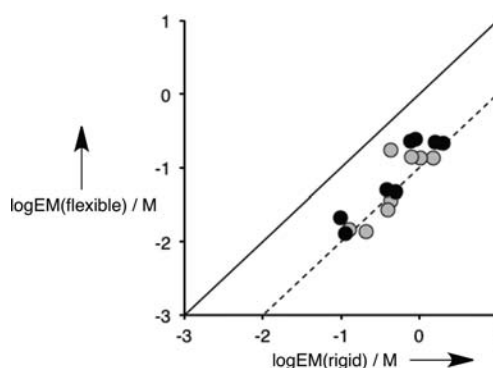
<sup>a</sup>Average error over the data set  $\pm 50\%$ . <sup>b</sup>No interaction detected.**Figure 12.** Comparison of effective molarities (EM) for formation of intramolecular H-bonds in toluene with the corresponding values measured in TCE for ester (black) and amide (gray) ligands. The line corresponds to  $\log EM(\text{TCE}) = \log EM(\text{toluene})$ .**Figure 13.** Comparison of effective molarities (EM) for formation of intramolecular H-bonds for ester ligands with the corresponding values measured for amide ligands in toluene (gray) and in TCE (black). The line corresponds to  $\log EM(\text{amide}) = \log EM(\text{ester})$ .

There is extremely good agreement between the two data sets. We have previously measured a number of ether–phenol H-bonds and phosphonate diester–phenol H-bonds in the same solvents using a closely related family of complexes. For ether–phenol H-bonds the results were similar to those reported here:

the EM was independent of solvent.<sup>9</sup> However, for phosphonate diester–phenol H-bonds, the value of EM changed by up to an order of magnitude in different solvents.<sup>9</sup> The results presented here suggest that the behavior of the phosphonate diester ligands is anomalous, which may be related to their steric bulk.<sup>9</sup>

Figure 13 compares that values of EM measured for the ester ligands with the values measured for the amide ligands, and again there is very good agreement between the two data sets. These results suggest that EM is a property of the supramolecular architecture and independent of the solvent and the intrinsic strength of the H-bonds involved.

Figure 14 compares the values of EM measured for the flexible ligands with values measured for the corresponding

**Figure 14.** Comparison of effective molarities (EM) measured for formation of intramolecular H-bonds for rigid ligands with the values measured for the corresponding flexible ligands in toluene (gray) and in TCE (black). The solid line corresponds to  $\log EM(\text{flexible}) = \log EM(\text{rigid})$ , and the dotted line corresponds to  $\log EM(\text{flexible}) = \log EM(\text{rigid}) - 1$ .

rigid ligands. Here there are substantial differences. The rigid ligands give values of EM that are approximately an order of magnitude higher than the values for the corresponding flexible ligands. This suggests that cost of restricting the conformational flexibility conferred by the additional rotor present in the flexible ligands is one order of magnitude in binding affinity.

## CONCLUSION

Comparison of the thermodynamic properties of a family of 64 closely related zinc porphyrin–pyridine ligand complexes that make intramolecular H-bonding interactions has allowed an evaluation of the effect of conformational flexibility on cooperativity in supramolecular complexes. Chemical double mutant cycles were used to measure the free energy contributions of intramolecular H-bonding interactions in 64 different systems. The results show that free energy contributions from intramolecular H-bonds make an additive contribution to the overall stability of the complex: the values of  $\Delta\Delta G^\circ$  for two-armed ligands are double the values for the corresponding one-armed ligands.

Comparison of the properties of the corresponding intermolecular H-bonds with the DMC results provides the values of EM for the intramolecular interactions in these systems. The value of EM for an ester–phenol H-bond is practically identical to the EM for the corresponding amide–phenol H-bond embedded in the same supramolecular architecture. The values of EM are also independent of the solvent, with similar results obtained in toluene and in TCE.

However, significant differences in EM are observed for rigid and flexible ligands. These two families of ligand have identical

H-bond donors at identical locations on the ligand framework, but the flexible ligands have one more torsional degree of freedom than the rigid ligands. The complexes formed with the rigid ligands are more stable than the complexes formed with the flexible ligands, and there is an order of magnitude difference in the value of EM. Although there are some conformational differences between the flexible and rigid, and amide and ester ligands, the results for different supramolecular architectures with different degrees of receptor–ligand complementarity are similar, which suggests that the results have general applicability. These experiments show that the cost of restricting a rotor in formation of a supramolecular complex is about 5 kJ/mol, which is comparable to the value found for intramolecular covalent interactions.

Previous estimates of the cost of restricting a rotor in a non-covalent complex are as high as 9 kJ/mol, which suggests that not all of the conformational entropy is frozen out in the formation of the H-bonded complexes described here, and higher EMs might be possible in more constrained systems.<sup>14</sup> The highest value of EM measured for complexes reported in this paper is 2 M, and Anderson has shown that it is possible to obtain an EM 3 orders of magnitude larger in a very highly organized system.<sup>15</sup>

## EXPERIMENTAL SECTION

**Synthesis. 3-(Pyridin-3-yl)benzoic Acid, 12 3.** To 3-bromopyridine (0.190 mL, 2.0 mmol), 3-carboxyphenylboronic acid (0.330 g, 2.00 mmol), and Pd(0)(PPh<sub>3</sub>)<sub>4</sub> (0.12g, 0.1 mmol), protected by an argon atmosphere, were added 0.4 M sodium carbonate<sub>(aq)</sub> (10 mL) and acetonitrile (10 mL). The mixture was heated at 90 °C for 36 h and allowed to cool. The volume was reduced by 50% under reduced pressure, washed with DCM (10 mL), and filtered. The product was precipitated from the aqueous layer with HCl<sub>(gas)</sub>. The product was purified on silica, eluting with EtOAc:AcOH. The product was isolated as a white solid: yield 0.087 g (22%); <sup>1</sup>H NMR (250 MHz, CDCl<sub>3</sub>) δ 9.29 (s, 1H), 9.02 (d, 1H, J = 8), 8.92 (d, 1H, J = 6), 8.49 (s, 1H), 8.27–8.22 (m, 2H), 8.10 (d, 1H, J = 8), 7.75 (dd, 1H, J = 8).

**3,3'-(Pyridine-3,5-diyl)dibenzoic Acid, 4.** To 3,5-dibromopyridine (0.236 g, 1.0 mmol), 3-carboxyphenylboronic acid (0.330 g, 2.00 mmol), and Pd(0)(PPh<sub>3</sub>)<sub>4</sub> (0.12g, 0.1 mmol), protected by an argon atmosphere, were added 0.4 M sodium carbonate<sub>(aq)</sub> (10 mL) and acetonitrile (10 mL). The mixture was heated at 90 °C for 36 h and allowed to cool. The volume was reduced by 50% under reduced pressure, washed with DCM (10 mL), and filtered. The product was precipitated from the aqueous layer with HCl<sub>(gas)</sub> and washed with water (2 mL). The product was isolated as a white solid: yield 0.297 g (93%); <sup>1</sup>H NMR (250 MHz, CDCl<sub>3</sub>) δ 9.14 (s, 2H), 8.84 (s, 1H), 8.43 (s, 2H), 8.20 (d, 2H, J = 8), 8.08 (d, 2H, J = 8), 7.71 (dd, 2H, J = 8); <sup>13</sup>C NMR (62.9 MHz, d<sub>5</sub>-DMSO) δ<sub>C</sub> = 167.48, 141.61, 139.51, 137.93, 135.50, 132.61, 132.28, 130.60, 130.18, 128.84; MS (ES+) *m/z* (%) = 320, [M+H<sup>+</sup>] (100); HRMS (ES+) calcd for C<sub>19</sub>H<sub>14</sub>NO<sub>4</sub> 320.0923, found 320.0921; FT-IR (thin film) ν<sub>max</sub>/cm<sup>-1</sup> 3034, 2965, 2858, 1682, 1569, 1463, 1432, 1397, 1303, 1262.

**Ligand L7e.** To 3 (0.087 g, 0.321 mmol) were added toluene (2 mL), SOCl<sub>2</sub> (6 mL) and DMF (10 μL). The mixture was refluxed for 1 h, protected by a CaCl<sub>2</sub> drying tube. The reaction was allowed to cool, solvent was removed under reduced pressure, and the residue was re-dissolved in DCM (25 mL). To this solution stirring at 0 °C, protected by a nitrogen atmosphere, was added diethylamine (0.212 mL, 2.96 mmol) in small portions. After 24 h the DCM solution was washed with 10% NaHCO<sub>3</sub>(aq) (2 × 10 mL) and brine (10 mL) and then dried with Na<sub>2</sub>SO<sub>4</sub>, the solvent was removed under reduced pressure, and the residue was purified on silica, eluting with EtOAc:hexane. The product was isolated as a clear oil: yield 0.060 g (70%); <sup>1</sup>H NMR (250 MHz, CDCl<sub>3</sub>) δ 8.86 (s, 1H), 8.63 (s, 1H), 7.90 (d, 1H, J = 8), 7.64–7.50 (m, 3H), 7.43–7.37 (m, 2H), 3.45 (d, 4H, J = 70), 1.22 (d, 6H, J = 30); <sup>13</sup>C NMR (100.6 MHz, CDCl<sub>3</sub>) δ<sub>C</sub> = 170.76, 148.78, 148.23, 138.17, 138.15,

135.97, 134.38, 129.18, 127.80, 125.84, 125.07, 123.63, 43.33, 39.31, 14.26, 12.67; MS (ES+) *m/z* (%) = 255 [M+H<sup>+</sup>] (100); HRMS (ES+) calcd for C<sub>16</sub>H<sub>19</sub>N<sub>2</sub>O 255.1497, found 255.1492; FT-IR (thin film) ν<sub>max</sub>/cm<sup>-1</sup> 2978, 2934, 2874, 1625, 1457, 1428, 1381, 1366, 1319, 1278, 1218, 1102.

**Ligand L8e.** To 4 (0.297 g, 0.835 mmol) was added toluene (5 mL), SOCl<sub>2</sub> (15 mL), and DMF (10 μL). The mixture was refluxed for 1 h, protected by a CaCl<sub>2</sub> drying tube. The reaction was allowed to cool, solvent was removed under reduced-pressure, and the residue was re-dissolved in DCM (50 mL). To this solution stirring at 0 °C, protected by a nitrogen atmosphere, was added diethylamine (0.616 mL, 6.68 mmol) in small portions. After 24 h the DCM solution was washed with 10% NaHCO<sub>3</sub>(aq) (2 × 20 mL) and brine (20 mL) and then dried with Na<sub>2</sub>SO<sub>4</sub>, the solvent was removed under reduced pressure, and the residue was purified on silica, eluting with EtOAc:hexane. The product was isolated as a clear oil: yield 0.325 g (90%); <sup>1</sup>H NMR (250 MHz, CDCl<sub>3</sub>) δ 8.85 (s, 2H), 8.07 (s, 1H), 7.70–7.66 (m, 4H), 7.55, (dd, 2H, J = 8, J = 8), 7.43 (d, 2H, J = 8), 3.46 (d, 8H, J = 70), 1.22 (d, 12H, J = 30); <sup>13</sup>C NMR (62.9 MHz, CDCl<sub>3</sub>) δ<sub>C</sub> = 170.74, 147.26, 138.34, 137.96, 136.02, 132.93, 129.27, 27.90, 126.02, 125.25, 43.59, 39.53, 14.46, 13.33; MS (ES+) *m/z* (%) = 430, [M+H<sup>+</sup>] (100); HRMS (ES+) calcd for C<sub>27</sub>H<sub>32</sub>N<sub>2</sub>O<sub>2</sub> 430.2495, found 430.2482; FT-IR (thin film) ν<sub>max</sub>/cm<sup>-1</sup> 2975, 2937, 2874, 1626, 1472, 1457, 1436, 1384, 1284, 1102.

**Ligand L7f.** To 3-(ethoxycarbonyl)phenylboronic acid (0.513 g, 2.64 mmol), Pd(0)(PPh<sub>3</sub>)<sub>4</sub> (0.0449g, 0.0387 mmol), and sodium carbonate (0.342, 3.23 mmol), protected by an argon atmosphere, were added THF (25 mL), toluene (25 mL), water (1 mL), and 3-bromopyridine (0.251 mL, 2.58 mmol). The mixture was heated at 90 °C for 36 h and allowed to cool, and the solvent was removed under reduced pressure. The solid was re-dissolved in DCM (50 mL), washed with 10% NaHCO<sub>3</sub>(aq) (20 mL) and brine (20 mL), and then dried with Na<sub>2</sub>SO<sub>4</sub>, the solvent was removed under reduced pressure, and the residue was purified on silica, eluting with EtOAc:hexane. The product was isolated as a clear oil: yield 0.15 g (27%); <sup>1</sup>H NMR (250 MHz, CDCl<sub>3</sub>) δ 8.85 (s, 1H), 8.59 (d, 1H, J = 5), 8.23 (s, 1H), 8.05 (d, 1H, J = 8), 7.87 (d, 1H, J = 8), 7.73 (d, 1H, J = 8), 7.52 (dd, 1H, J = 8, J = 8), 7.35 (dd, 1H, J = 5, J = 8), 4.38 (q, 2H, J = 7), 1.39 (t, 3H, J = 7); <sup>13</sup>C NMR (100.6 MHz, CDCl<sub>3</sub>) δ<sub>C</sub> = 166.21, 148.88, 148.26, 138.09, 135.73, 134.42, 131.43, 131.32, 129.14, 129.11, 128.21, 123.62, 61.21, 14.32; MS (ES+) *m/z* (%) = 228 [M+H<sup>+</sup>] (100); HRMS (ES+) calcd for C<sub>14</sub>H<sub>14</sub>NO<sub>2</sub> 228.1025, found 228.1025; FT-IR (thin film) ν<sub>max</sub>/cm<sup>-1</sup> 3037, 2983, 2936, 2904, 1718, 1470, 1437, 1369, 1308, 1251, 1114, 1085.

**Ligand L8f.** To 3-(ethoxycarbonyl)phenylboronic acid (0.513 g, 2.64 mmol), Pd(0)(PPh<sub>3</sub>)<sub>4</sub> (0.0449g, 0.0387 mmol), sodium carbonate (0.342, 3.23 mmol) and 3,5-dibromopyridine (0.306 g, 1.29 mmol), protected by an argon atmosphere, were added THF (25 mL), toluene (25 mL), and water (1 mL). The mixture was heated at 90 °C for 36 h and then allowed to cool, and the solvent was removed under reduced pressure. The solid was re-dissolved in DCM (50 mL), washed with 10% NaHCO<sub>3</sub>(aq) (20 mL) and brine (20 mL), and dried with Na<sub>2</sub>SO<sub>4</sub>, the solvent was removed under reduced pressure, and the residue was purified on silica, eluting with EtOAc:hexane. The product was isolated as a white solid: yield 0.211 g (45%); mp = 104–106 °C; <sup>1</sup>H NMR (250 MHz, CDCl<sub>3</sub>) δ 8.88 (s, 2H), 8.33 (s, 2H), 8.12 (d, 2H, J = 6), 8.12 (d, 2H, J = 7), 8.11 (s, 1H), 7.59 (dd, 2H, J = 8, J = 8), 4.43 (q, 4H, J = 7), 1.43 (t, 6H, J = 7); <sup>13</sup>C NMR (62.9 MHz, CDCl<sub>3</sub>) δ<sub>C</sub> = 166.22, 147.38, 137.82, 135.89, 133.03, 131.55, 131.48, 129.38, 129.27, 128.34, 61.37, 14.37; MS (ES+) *m/z* (%) = 376, [M+H<sup>+</sup>] (80), 382, (100), 425 (90); HRMS (ES+) calcd for C<sub>23</sub>H<sub>22</sub>NO<sub>4</sub> 376.1549, found 376.1560.

**Ligand L2e.** A mixture of nicotinic acid (1 g, 8.12 mmol), toluene (10 mL), DMF (10 μL), and thionyl chloride (30 mL) was refluxed for 1 h, protected by a CaCl<sub>2</sub> drying tube. The solvent was removed on a rotary evaporator, and the residue was dissolved in DCM (20 mL). *N,N*-Diethyl-2-hydroxyacetamide (1.3 mL, 10.3 mmol) was added in small portions, and then triethylamine (2.46 mL, 24.4 mmol) was added dropwise. The solution was allowed to stir 18 h at room temperature. After dilution with DCM (20 mL), the solution was washed with aqueous NaHCO<sub>3</sub>(aq) (10% w/v) (1 × 40 mL) and brine (1 × 40 mL)

and dried with  $\text{MgSO}_4$ . The solvent was removed on a rotary evaporator, and the crude product was purified on silica, eluting with EtOAc:hexane. The product was isolated as a white solid: yield 1.52 g (79%); mp = 65–66 °C;  $^1\text{H}$  NMR (250 MHz,  $\text{CDCl}_3$ )  $\delta$  9.17 (s, 1H), 8.66 (d, 1H,  $J$  = 5), 8.24 (d, 1H,  $J$  = 8), 7.28 (dd, 1H,  $J$  = 8,  $J$  = 5), 4.88 (s, 2H), 3.29 (q, 2H,  $J$  = 7), 3.19 (q, 2H,  $J$  = 7), 1.13 (t, 3H,  $J$  = 7), 1.01 (t, 3H,  $J$  = 7);  $^{13}\text{C}$  NMR (62.9 MHz,  $\text{CDCl}_3$ )  $\delta_{\text{C}}$  = 164.91, 164.91, 153.52, 151.01, 137.23, 125.54, 123.22, 61.91, 40.87, 40.39, 14.06, 12.80; MS (ES+)  $m/z$  (%) = 237 [ $\text{M}+\text{H}^+$ ] (100), 259 [ $\text{M}+\text{Na}^+$ ] (20); HRMS (ES+) calcd for  $\text{C}_{12}\text{H}_{17}\text{N}_2\text{O}_3$  237.1239, found 237.1229; FT-IR (thin film)  $\nu_{\text{max}}/\text{cm}^{-1}$  3098, 3060, 2980, 2964, 2944, 2903, 1735, 1651, 1472, 1423, 1295, 1269, 1119.

**Ligand L3e.** A mixture of 3,5-pyridinedicarboxylic acid (1 g, 5.98 mmol), toluene (20 mL), dimethylformamide (20  $\mu\text{L}$ ), and thionyl chloride (30 mL) was refluxed for 1 h, protected by a  $\text{CaCl}_2$  drying tube. The solvent was removed on a rotary evaporator and the residue was dissolved in dichloromethane (20 mL). *N,N*-Diethyl-2-hydroxyacetamide (1.87 mL, 14.35 mmol) was added in small portions, and then triethylamine (1.82 mL, 17.9 mmol) was added dropwise. The solution was allowed to stir 18 h at room temperature. After dilution with DCM (20 mL), the solution was washed with  $\text{NaHCO}_3(\text{aq})$  (10% w/v) (40 mL) and brine (40 mL) and dried with  $\text{MgSO}_4$ . The solvent was removed on a rotary evaporator and the crude product was purified on silica eluting with EtOAc:MeOH. The product was isolated as white solid: yield 1.95 g (83%). Mp = 103–104 °C  $^1\text{H}$  NMR (250 MHz,  $\text{CDCl}_3$ )  $\delta$  9.44 (s, 2H), 9.01 (s, 1H), 5.00 (s, 4H), 3.40 (q, 4H,  $J$  = 7), 3.30 (q, 4H,  $J$  = 7), 1.26 (t, 6H,  $J$  = 7), 1.14 (t, 6H,  $J$  = 7);  $^{13}\text{C}$  NMR (62.9 MHz,  $\text{CDCl}_3$ )  $\delta_{\text{C}}$  = 164.74, 164.19, 154.70, 138.65, 125.57, 62.20, 40.99, 40.55, 14.18, 12.89; MS (ES+)  $m/z$  (%) = 394 [ $\text{M}+\text{H}^+$ ] (100); HRMS (ES+) calcd for  $\text{C}_{19}\text{H}_{28}\text{N}_3\text{O}_6$  394.1978, found 394.1972; FT-IR (thin film)  $\nu_{\text{max}}/\text{cm}^{-1}$  3082, 3037, 2967, 2932, 1725, 1671, 1651, 1465, 1449, 1430, 1234, 1218, 1103, 1042, 1026.

**Ligand L2f.** A mixture of nicotinic acid (1 g, 8.12 mmol), toluene (10 mL), DMF (10  $\mu\text{L}$ ), and thionyl chloride (30 mL) was refluxed for 1 h, protected by a  $\text{CaCl}_2$  drying tube. The solvent was removed on a rotary evaporator, and the residue was dissolved in DCM (20 mL). Ethyl glycolate (0.97 mL, 10.3 mmol) was added in small portions, and then triethylamine (2.46 mL, 24.4 mmol) was added dropwise. The solution was allowed to stir 18 h at room temperature. After dilution with DCM (20 mL), the solution was washed with  $\text{NaCO}_3(\text{aq})$  (10% w/v) (40 mL) and brine (40 mL) and dried with  $\text{MgSO}_4$ . The solvent was removed on a rotary evaporator, and the crude product was purified on silica, eluting with EtOAc:hexane. The product was isolated as clear oil: yield 1.27 g (75%);  $^1\text{H}$  NMR (250 MHz,  $\text{CDCl}_3$ )  $\delta$  9.14 (s, 1H), 8.67 (d, 1H,  $J$  = 5), 8.21 (d, 1H,  $J$  = 8), 7.29 (dd, 1H,  $J$  = 8,  $J$  = 5), 4.76 (s, 2H), 4.12 (q, 2H,  $J$  = 7), 1.15 (t, 3H,  $J$  = 7);  $^{13}\text{C}$  NMR (62.9 MHz,  $\text{CDCl}_3$ )  $\delta_{\text{C}}$  = 167.26, 164.53, 153.72, 150.95, 137.16, 125.15, 123.27, 61.44, 61.26, 13.96; MS (ES+)  $m/z$  (%) = 210 [ $\text{M}+\text{H}^+$ ] (100); HRMS (ES+) calcd for  $\text{C}_{10}\text{H}_{12}\text{NO}_4$  210.0766, found 210.0768; FT-IR (thin film)  $\nu_{\text{max}}/\text{cm}^{-1}$  3024, 2984, 1732, 1590, 1423, 1383, 1295, 1215, 1124, 1117, 1030, 749.

**Ligand L3f.** A mixture of 3,5-pyridinedicarboxylic acid (1 g, 5.98 mmol), toluene (20 mL), DMF (20  $\mu\text{L}$ ), and thionyl chloride (30 mL) was refluxed for 1 h, protected by a  $\text{CaCl}_2$  drying tube. The solvent was removed on a rotary evaporator, and the residue was dissolved in DCM (20 mL). Ethyl glycolate (1.48 mL, 14.35 mmol) was added in small portions, and then triethylamine (1.82 mL, 17.9 mmol) was added dropwise. The solution was allowed to stir for 18 h at room temperature. After dilution with DCM (20 mL), the solution was washed with  $\text{NaHCO}_3(\text{aq})$  (10% w/v) (1  $\times$  40 mL) and brine (1  $\times$  40 mL) and dried with  $\text{MgSO}_4$ . The solvent was removed on a rotary evaporator, and the crude product was purified on silica, eluting with EtOAc:hexane. The product was isolated as waxy solid: yield 1.74 g (86%); mp = 41–43 °C;  $^1\text{H}$  NMR (250 MHz,  $\text{CDCl}_3$ )  $\delta$  9.41 (s, 2H), 8.94 (s, 1H), 4.88 (s, 2  $\times$  2H), 4.24 (q, 2  $\times$  2H,  $J$  = 7), 1.27 (t, 2  $\times$  3H,  $J$  = 7);  $^{13}\text{C}$  NMR (62.9 MHz,  $\text{CDCl}_3$ )  $\delta_{\text{C}}$  = 167.09, 163.73, 154.77, 138.53, 125.29, 61.68, 61.57, 14.07; MS (ES+)  $m/z$  (%) = 340 [ $\text{M}+\text{H}^+$ ] (100); HRMS (ES+) calcd for  $\text{C}_{15}\text{H}_{18}\text{NO}_8$  340.1032, found 340.1019; FT-IR (thin film)  $\nu_{\text{max}}/\text{cm}^{-1}$  3069, 3018, 2980, 2938, 1735, 1600, 1430, 1379, 1276, 1205, 1103, 1035, 1013.

**Ligand L7c.** To *m*-tolylboronic acid (0.359 g, 2.64 mmol),  $\text{Pd}(\text{O})(\text{PPh}_3)_4$  (0.0449g, 0.0387 mmol), and sodium carbonate (0.342, 3.23 mmol), protected by an argon atmosphere, were added THF (25 mL), toluene (25 mL), water (1 mL), and 3-bromopyridine (0.251 mL, 2.58 mmol). The mixture was heated at 105 °C for 24 h and then allowed to cool, and the solvent was removed under reduced pressure. The solid was re-dissolved in DCM (50 mL), washed with 10%  $\text{NaHCO}_3(\text{aq})$  (20 mL) and brine (20 mL), and then dried with  $\text{Na}_2\text{SO}_4$ , the solvent was removed under reduced pressure, and the residue was purified on silica, eluting with EtOAc:hexane. The product was isolated as a clear oil: yield 0.256 g (59%);  $^1\text{H}$  NMR (250 MHz,  $\text{CDCl}_3$ )  $\delta$  8.86 (s, 1H), 8.60 (d, 1H,  $J$  = 5), 7.87 (d, 1H,  $J$  = 8), 7.40–7.33 (m, 4H), 7.24 (d, 1H,  $J$  = 4), 2.45 (s, 3H);  $^{13}\text{C}$  NMR (62.9 MHz,  $\text{CDCl}_3$ )  $\delta_{\text{C}}$  = 148.38, 148.35, 138.77, 137.82, 136.75, 134.38, 129.01, 128.87, 127.92, 124.27, 123.52, 21.55; MS (ES+)  $m/z$  (%) = 170 [ $\text{M}+\text{H}^+$ ] (100); HRMS (ES+) calcd for  $\text{C}_{12}\text{H}_{12}\text{N}$  170.0790, found 170.0966; FT-IR (thin film)  $\nu_{\text{max}}/\text{cm}^{-1}$  3028, 2955, 2922, 2862, 1610, 1592, 1575, 1474, 1435, 1403, 1338, 1188, 1100, 1022.

**Ligand L8c.** To *m*-tolylboronic acid (0.359 g, 2.64 mmol),  $\text{Pd}(\text{O})(\text{PPh}_3)_4$  (0.0449g, 0.0387 mmol), sodium carbonate (0.342 g, 3.23 mmol), and 3,5-dibromopyridine (0.306 g, 1.29 mmol), protected by an argon atmosphere, were added THF (25 mL), toluene (25 mL), and water (1 mL). This mixture was heated at 90 °C for 36 h and then allowed to cool, and the solvent was removed under reduced pressure. The solid was re-dissolved in DCM (50 mL), washed with 10%  $\text{NaHCO}_3(\text{aq})$  (20 mL) and brine (20 mL), and dried with  $\text{Na}_2\text{SO}_4$ , the solvent was removed under reduced pressure, and the residue was purified on silica, eluting with EtOAc:hexane. The product was isolated as a white solid: yield 0.082 g (24%); mp = 136–138 °C;  $^1\text{H}$  NMR (250 MHz,  $\text{CDCl}_3$ )  $\delta$  8.84 (s, 2H), 8.06 (s, 1H), 7.49–7.39 (m, 6H), 7.28 (d, 2H,  $J$  = 8), 2.48 (s, 6H);  $^{13}\text{C}$  NMR (62.9 MHz,  $\text{CDCl}_3$ )  $\delta_{\text{C}}$  = 146.97, 138.83, 137.80, 136.72, 132.95, 129.05, 128.98, 128.04, 124.40, 21.58; MS (ES+)  $m/z$  (%) = 260, [ $\text{M}+\text{H}^+$ ] (100); HRMS (ES+) calcd for  $\text{C}_{19}\text{H}_{18}\text{N}$  260.1439, found 260.1438.

***N,N*-Diethyl-4-methylbenzamide, 5.** To 4-methylbenzoyl chloride (5 g, 32.3 mmol) stirring at 0 °C, protected by an  $\text{N}_2$  atmosphere, was added diethylamine (16.8 mL, 162 mmol) in small portions. After 24 h the DCM solution was washed with 10%  $\text{NaHCO}_3(\text{aq})$  (2  $\times$  30 mL) and brine (30 mL) and then dried with  $\text{Na}_2\text{SO}_4$ , the solvent was removed under reduced pressure, and the residue was purified on silica, eluting with EtOAc:hexane. The product was isolated as a clear oil: yield 4.36 g (71%);  $^1\text{H}$  NMR (250 MHz,  $\text{CDCl}_3$ )  $\delta$  7.25 (d, 2H,  $J$  = 8), 7.16 (d, 2H,  $J$  = 8), 3.38 (d, 4H,  $J$  = 30), 2.34 (s, 3H), 1.15 (s, 6H);  $^{13}\text{C}$  NMR (100.6 MHz,  $\text{CDCl}_3$ )  $\delta_{\text{C}}$  = 171.46, 139.03, 134.38, 138.95, 126.31, 49.30, 39.21, 21.32, 14.23, 12.92; MS (ES+)  $m/z$  (%) = 192 [ $\text{M}+\text{H}^+$ ] (100); HRMS (ES+) calcd for  $\text{C}_{12}\text{H}_{18}\text{NO}$  192.1388, found 192.1390; FT-IR (thin film)  $\nu_{\text{max}}/\text{cm}^{-1}$  2972, 2937, 2879, 1630, 1514, 1466, 1428, 1381, 1365, 1313, 1293, 1214, 1096.

**UV/Visible Absorption and Fluorescence Titrations.** UV/vis titrations were carried out by preparing a 10 mL sample of porphyrin at known concentration (4–7  $\mu\text{M}$ ) in spectroscopic-grade solvent. A 10 mL solution of ligand (12–3900  $\mu\text{M}$ ) was prepared using spectroscopic-grade solvent. To a Hellma quartz 96-well plate was added 150  $\mu\text{L}$  of porphyrin solution, and the UV/vis absorbance was recorded at five wavelengths. Aliquots of pyridine solution (3, 6, or 10  $\mu\text{L}$ ) were added successively to the well containing the porphyrin solution, using the BMG FLUOstar Omega plate reader, and the plate was equilibrated at 298 K. For absorption experiments, the UV/vis absorbance was recorded at five wavelengths after each addition. For emission experiments, the plate was excited at 420 or 430 nm, and the fluorescence emission was recorded at four wavelengths after each addition. Changes in absorbance or emission were fit to a 1:1 binding isotherm in Microsoft Excel to obtain the association constant. Each titration was repeated at least three times, and the experimental error is quoted as twice the standard deviation at a precision of one significant figure.

**ITC Measurements.** ITC experiments were performed at 298 K on a VP-ITC MicroCal titration calorimeter (MicroCal, Inc., Northampton, MA). In a typical calorimetric measurement, porphyrin host was dissolved in HPLC-grade solvents at concentrations of 0.5–50  $\mu\text{M}$ , and the solution was loaded into the sample cell of the microcalorimeter.

The ligand guest solutions, 15–20 times more concentrated than the host solution, were loaded into the injection syringe. The number of injections was 30–50, and the volumes of the injections were between 7 and 10  $\mu\text{L}$ , with 30–60 s of duration and 300 s of spacing between the injections. The dilution experiments were performed for each titration, loading the guest solution at the same concentration as for the host titration into the injection syringe, and adding guest to the solvent in the cell. The dilution data were subtracted from each host titration thermogram. The data fitting was performed by using ORIGIN (Version 7.0, Microcal, LLC ITC) and a 1:1 binding isotherm (One Set of Sites model), allowing the stoichiometry number, the stability constant  $K$ , and the binding enthalpy  $\Delta H$  values to float. At least two independent measurements were performed for each host–guest system.

**NMR Titrations.** NMR titrations were carried out by preparing a 2 mL sample of host at known concentration (8–60 mM). Then, 0.6 mL of this solution was removed, and a  $^1\text{H}$  NMR spectrum was recorded. A solution of guest (12–1400 mM) was prepared by dissolving the guest in 1 mL of the host solution, so that the concentration of host remained constant throughout the titration. Aliquots of guest solution were added successively to the NMR tube containing the host, and the NMR spectrum was recorded after each addition. Changes in chemical shift were fit to a 1:1 binding isotherm in Microsoft Excel. Each titration was repeated at least three times, and the experimental error is quoted as twice the standard deviation at a precision of one significant figure.

## ■ ASSOCIATED CONTENT

### ● Supporting Information

CIF file for the X-ray crystal structure of the **P1a·L8f** complex. This material is available free of charge via the Internet at <http://pubs.acs.org>.

## ■ AUTHOR INFORMATION

### Corresponding Author

c.hunter@sheffield.ac.uk

### Notes

The authors declare no competing financial interest.

## ■ ACKNOWLEDGMENTS

We thank the EPSRC and Royal Society for funding and the National Crystallographic Service at the University of Southampton for collecting X-ray data.

## ■ REFERENCES

- (1) (a) Badjic, J. D.; Nelson, A.; Cantrill, S. J.; Turnbull, W. B.; Stoddart, J. F. *Acc. Chem. Res.* **2005**, *38*, 723–732. (b) Doyle, A. G.; Jacobsen, E. N. *Chem. Rev.* **2007**, *107*, 5713–5743. (c) Kay, E. R.; Leigh, D. A.; Zerbetto, F. *Angew. Chem., Int. Ed.* **2007**, *46*, 72–191. (d) Lehn, J. M. *Angew. Chem., Int. Ed.* **1990**, *29*, 1304–1319. (e) Philp, D.; Stoddart, J. F. *Angew. Chem., Int. Ed.* **1996**, *35*, 1155–1196. (f) Mulder, A.; Huskens, J.; Reinhoudt, D. N. *Org. Biomol. Chem.* **2004**, *2*, 3409–3424. (g) Williams, D. H.; Bardsley, B. *Angew. Chem., Int. Ed.* **1999**, *38*, 1173–1193. (h) Mammen, M.; Choi, S. K.; Whitesides, G. M. *Angew. Chem., Int. Ed.* **1998**, *37*, 2755–2794. (i) Takeuchi, M.; Ikeda, M.; Sugasaki, A.; Shinkai, S. *Acc. Chem. Res.* **2001**, *34*, 865–873. (j) O'Sullivan, M. C.; Sprafke, J. K.; Kondratuk, D. V.; Rinfrey, C.; Claridge, T. D. W.; Saywell, A.; Blunt, M. O.; O'Shea, J. N.; Beton, P. H.; Malfois, M.; Anderson, H. L. *Nature* **2011**, *469*, 72–75.
- (2) (a) Andrews, P. R.; Craik, D. J.; Martin, J. L. *J. Med. Chem.* **1984**, *27*, 1648–1657. (b) Free, S. M.; Wilson, J. W. *J. Med. Chem.* **1964**, *7*, 395. (c) Gohlke, H.; Klebe, G. *Angew. Chem., Int. Ed.* **2002**, *41*, 2645–2676. (d) Tomic, S.; Nilsson, L.; Wade, R. C. *J. Med. Chem.* **2000**, *43*, 1780–1792. (e) Hunter, C. A. *Angew. Chem., Int. Ed.* **2004**, *43*, 5310–5324.
- (3) Kirby, A. J. *Adv. Phys. Org. Chem.* **1980**, *17*, 183.
- (4) Galli, C.; Mandolini, L. *Eur. J. Org. Chem.* **2000**, 3117–3125.

- (5) (a) Bruice, T. C.; Lightstone, F. C. *Acc. Chem. Res.* **1999**, *32*, 127–136. (b) Bruice, T. C.; Pandit, U. K. *J. Am. Chem. Soc.* **1960**, *82*, 5858–5865. (c) Page, M. L.; Jencks, W. P. *Proc. Natl. Acad. Sci. U.S.A.* **1971**, *68*, 1678.

- (6) (a) Hunter, C. A.; Ihekwaba, N.; Misuraca, M. C.; Segarra-Maset, M. D.; Turega, S. M. *Chem. Commun.* **2009**, 26, 3964–3966. (b) Lemonnier, J. F.; Guenee, L.; Bernardinelli, G.; Vigier, J. F.; Bocquet, B.; Piguat, C. *Inorg. Chem.* **2010**, *49*, 1252–1265. (c) Tobey, S. L.; Anslyn, E. V. *J. Am. Chem. Soc.* **2003**, *125*, 10963–10970. (d) Williams, D. H.; Davies, N. L.; Zerella, R.; Bardsley, B. *J. Am. Chem. Soc.* **2004**, *126*, 2042–2049. (e) Kondratuk, D. V.; Perdigao, L. M. A.; O'Sullivan, M. C.; Svatek, S.; Smith, G.; O'Shea, J. N.; Beton, P. H.; Anderson, H. L. *Angew. Chem., Int. Ed.* **2012**, *51*, 6696–6699.

- (7) (a) Krishnamurthy, V. M.; Semetey, V.; Bracher, P. J.; Shen, N.; Whitesides, G. M. *J. Am. Chem. Soc.* **2007**, *129*, 1312–1320. (b) Hossain, M. A. S.; Schneider, H. J. *Chem.—Eur. J.* **1999**, *5*, 1284–1290. (c) ten Cate, A. T.; Kooijman, H.; Spek, A. L.; Sijbesma, R. P.; Meijer, E. W. *J. Am. Chem. Soc.* **2004**, *126*, 3801–3808. (d) Jiang, W.; Nowosinski, K.; Loew, N. L.; Dzyuba, E. V.; Klautzsch, F.; Schaefer, A.; Huuskonen, J.; Rissanen, K.; Schalley, C. A. *J. Am. Chem. Soc.* **2012**, *134*, 1860–1868. (e) Misuraca, M. C.; Grecu, T.; Freixa, Z.; Garavini, V.; Hunter, C. A.; van Leeuwen, P.; Segarra-Maset, M. D.; Turega, S. M. *J. Org. Chem.* **2011**, *76*, 2723–2732. (f) Searle, M. S.; Williams, D. H. *J. Am. Chem. Soc.* **1992**, *114*, 10690–10697. (g) Searle, M. S.; Williams, D. H.; Gerhard, U. *J. Am. Chem. Soc.* **1992**, *114*, 10697–10704. (h) Bohm, H. J. *J. Comput.-Aided Mol. Des.* **1994**, *8*, 243–256. (i) Nangreave, J.; Yan, H.; Liu, Y. *J. Am. Chem. Soc.* **2011**, *133*, 4490–4497.

- (8) (a) Gunasekaran, K.; Nussinov, R. *J. Mol. Biol.* **2007**, *365*, 257–273. (b) Jimenez, R.; Salazar, G.; Baldrige, K. K.; Romesberg, F. E. *Proc. Natl. Acad. Sci. U.S.A.* **2003**, *100*, 92–97. (c) Shi, R.; Munger, C.; Kalan, L.; Sulea, T.; Wright, G. D.; Cygler, M. *Proc. Natl. Acad. Sci. U.S.A.* **2012**, *109*, 11824–11829. (d) Sohtome, Y.; Nagasawa, K. *Chem. Commun.* **2012**, 48, 7777–7789. (e) Pearson, R. J.; Kassianidis, E.; Slawin, A. M. Z.; Philp, D. *Chem.—Eur. J.* **2006**, *12*, 6829–6840.

- (9) (a) Chekmeneva, E.; Hunter, C. A.; Packer, M. J.; Turega, S. M. *J. Am. Chem. Soc.* **2008**, *130*, 17718–17725. (b) Hunter, C. A.; Misuraca, M. C.; Turega, S. M. *J. Am. Chem. Soc.* **2011**, *133*, 582–594. (c) Hunter, C. A.; Misuraca, M. C.; Turega, S. M. *J. Am. Chem. Soc.* **2011**, *133*, 20416–20425. (d) Hunter, C. A.; Misuraca, M. C.; Turega, S. M. *Chem. Sci.* **2012**, *3*, 589–601. (e) Hunter, C. A.; Misuraca, M. C.; Turega, S. M. *Chem. Sci.* **2012**, *3*, 2462–2469. (f) Chekmeneva, E.; Hunter, C. A.; Misuraca, M. C.; Turega, S. M. *Org. Biomol. Chem.* **2012**, *10*, 6022–6031.

- (10) (a) Fersht, A. R.; Kirby, A. J. *J. Am. Chem. Soc.* **1967**, *89*, 4857. (b) Chi, X. L.; Guerin, A. J.; Haycock, R. A.; Hunter, C. A.; Sarson, L. D. *Chem. Commun.* **1995**, 2563–2565. (c) Cacciapaglia, R.; Di Stefano, S.; Mandolini, L. *Acc. Chem. Res.* **2004**, *37*, 113–122. (d) Ercolani, G.; Piguat, C.; Borkovec, M.; Hamacek, J. *J. Phys. Chem. B* **2007**, *111*, 12195–12203. (e) Sinclair, A. J.; del Amo, V.; Philp, D. *Org. Biomol. Chem.* **2009**, *7*, 3308–3318.

- (11) (a) Cockroft, S. L.; Hunter, C. A. *Chem. Soc. Rev.* **2007**, *36*, 172–188. (b) Camara-Campos, A.; Musumeci, D.; Hunter, C. A.; Turega, S. *J. Am. Chem. Soc.* **2009**, *131*, 18518–18524.

- (12) Gong, Y.; Pauls, H. W. *Synlett* **2000**, 6, 829–831.

- (13) (a) Abraham, M. H.; Grellier, P. L.; Prior, D. V.; Morris, J. J.; Taylor, P. J. *J. Chem. Soc., Perkin Trans. 2* **1990**, 521–529. (b) Abraham, M. H.; Platts, J. A. *J. Org. Chem.* **2001**, *66*, 3484–3491.

- (14) Ercolani, E. *Org. Lett.* **2005**, *7*, 803–805.

- (15) Hogben, H. J.; Sprafke, J. K.; Hoffmann, M.; Pawlicki, M.; Anderson, H. L. *J. Am. Chem. Soc.* **2011**, *133*, 20962–20969.